Journal of Controlled Release 237 (2016) 61–70

Contents lists available at ScienceDirect

Journal of Controlled Release

journal homepage: www.elsevier.com/locate/jconrel

Surface functionality affects the biodistribution and microglia-targeting of intra-amniotically delivered dendrimers☆

Fan Zhang [a,b], Elizabeth Nance [a,c,1], Zhi Zhang [c], Venkatasai Jasty [a], Siva P. Kambhampati [a,d], Manoj K. Mishra [a,d], Irina Burd [e], Roberto Romero [f], Sujatha Kannan [a,c,e,f,*], Rangaramanujam M. Kannan [a,b,c,d,f,**]

[a] Center for Nanomedicine at the Wilmer Eye Institute, Johns Hopkins University School of Medicine, Baltimore, MD 21231, United States
[b] Department of Materials Science, Johns Hopkins University, Baltimore, MD 21218, United States
[c] Anesthesiology and Critical Care Medicine, Johns Hopkins University School of Medicine, Baltimore, MD 21287, United States
[d] Department of Ophthalmology, Wilmer Eye Institute, Johns Hopkins University School of Medicine, Baltimore, MD 21231, United States
[e] Integrated Research Center for Fetal Medicine, Department of Gynecology and Obstetrics, Johns Hopkins University School of Medicine, Baltimore, MD 21287, United States
[f] Perinatology Research Branch, Detroit, MI 48201, United States

ARTICLE INFO

Article history:
Received 18 April 2016
Received in revised form 14 June 2016
Accepted 29 June 2016
Available online 1 July 2016

Keywords:
Dendrimer
Surface functionality
Intra-amniotic delivery
Blood-placental barrier
Microglia
Neuroinflammation

ABSTRACT

Cerebral Palsy (CP) is a chronic childhood disorder with limited therapeutic options. Maternal intrauterine inflammation/infection is a major risk factor in the pathogenesis of CP. In pre-clinical models, dendrimer-based therapies are viable in postnatal period, attenuating inflammation and improving motor function *in vivo*. However, treatment to the mother, in the prenatal period, may provide the possibility of preventing/resolving inflammation at early stages. Towards this goal, we used a maternal intrauterine inflammation-induced rabbit model of CP to study fetal-maternal transport and neuroinflammation targeting of intra-amniotically administrated dendrimers with neutral/anionic surface functionality. Our study suggested both hydroxyl-terminated 'neutral' (D-OH) and carboxyl-terminated 'anionic' (D-COOH) Polyamidoamine (PAMAM) dendrimers were absorbed by fetuses and demonstrated bi-directional transport between fetuses and mother. D-OH was more effective in crossing the fetal blood-brain barrier, and targeting activated microglia. The cell-specific targeting was associated with the extent of microglia activation. This study demonstrated intra-amniotically administered hydroxyl PAMAM dendrimers could be an effective drug delivery vehicle for targeting fetal inflammation and preventing subsequent neurologic injury associated with chorioamnionitis.

1. Introduction

Cerebral Palsy (CP) is a chronic childhood disorder caused by injury to the developing brain that occurs either *in utero*, during birth, or soon after birth [1]. As a result, patients usually develop permanent motor, sensory, and cognitive deficits [2]. According to the United States Centers for Disease Control and Prevention (CDC), the prevalence of CP is 1.5–4 per 1000 live births [3]. In infants born prematurely, 5–10% develop motor disability, and 40–50% develop some forms of cognitive and/or behavioral disability [4]. Although CP has multiple etiologies [5], a major pathological substrate is neuroinflammation mediated by activated microglia/astrocytes, leading to periventricular leukomalacia (PVL) [6]. Pro-inflammatory activation of microglial cells can result in persistent neuroinflammation, including release of free radicals, excitotoxic metabolites, and pro-inflammatory cytokines, leading to diffuse white and grey matter injury at foci where conventional therapeutics cannot reach and achieve cellular-targeting [7]. Therefore, an effective therapeutic agent should cross the blood-brain barrier (BBB), achieve rapid transport to reach the cells associated with inflammation and injury, and should avoid uptake by healthy cells/regions of the brain [8–10].

The pre-clinical success of *postnatal*, systemic Polyamidoamine (PAMAM) dendrimer-*N*-acetyl-L-cysteine conjugate (D-NAC) therapy suggests that there is a window of opportunity in the perinatal period for the treatment of neuroinflammation [11]. Treatment of the mother in the *prenatal* period is one such opportunity. However, the lack of studies on drug efficacies, kinetics of prenatal therapy and relative distribution between maternal and fetal compartments have limited the use of fetal therapies in the perinatal period. To achieve prenatal delivery of therapeutics to the fetus, intra-amniotic delivery is one possible administration route. Although delivery thorough amniotic fluid is a

☆ The authors disclose no potential conflicts of interest.

* Correspondence to: S. Kannan, 1800 Orleans Street, Suite 6318D, Baltimore, MD 21287, United States.
** Correspondence to: R.M. Kannan, 400 North Broadway, Smith building 6023, Baltimore, MD 21231, United States.
E-mail addresses: skannan3@jhmi.edu (S. Kannan), krangar1@jhmi.edu (R.M. Kannan).
[1] Present address: Department of Chemical Engineering, University of Washington, Seattle, WA, 98195-1750, United States.

http://dx.doi.org/10.1016/j.jconrel.2016.06.046
0168-3659/

unique delivery strategy, it amounts to oral delivery, as the fetus swallows the dendrimers along with amniotic fluid.

Recent *in vivo* studies on oral delivery of dendrimers showed dendrimers as promising intestinal penetration enhancers, drug solubilizers, and drug carriers [12–15]. Surface functionality plays a key role in the absorption of orally delivered dendrimers. Cationic dendrimers were not considered in this study due to their reported neural and systemic toxicity [16–18]. Although both hydroxyl-terminated neutral dendrimers (D-OH) and carboxyl-terminated anionic PAMAM dendrimers (D-COOH) were reported to show oral bioavailability, D-COOH achieved better oral bioavailability than D-OH [12–15], while maintaining a similar biosafety profile [19]. In addition, surface functionality of nanoparticles also determines their transport in the brain parenchyma. Neutrally charged nanoparticles demonstrated fast and deep brain tissue penetration either through intravenous [20,21], subarachnoid [22], or intracranial administration [23]. To efficiently target neuroinflammation in the CP model through intra-amniotic administration, understanding the role of dendrimer surface functionality on the fetal and brain uptake is critical.

In the present study, fetal uptake, cellular localization in the brain, and the bi-directional transport across the maternal-fetal compartment of intra-amniotically administered hydroxyl and carboxyl-functionalized PAMAM dendrimers were investigated.

2. Methods

2.1. Materials

Generation 4.0 Polyamidoamine (PAMAM) dendrimers with hydroxyl-terminated functional group (D-OH), and Generation 3.5 Polyamidoamine (PAMAM) dendrimers with carboxyl-terminated functional group (D-COOH) (Dendritech Inc.). Methanol (HPLC grade, Sigma-Aldrich), Cy5-NHS ester (GE Healthcare Life Science), stainless steel beads (Fisher Scientific), Fmoc-1,5-diaminopentane hydrobromide (Sigma), TSK gel ODS-80 Ts (250 4.6 mm, i.d., 5 μm) column (Tosoh Bioscience LLC, Japan), 4′,6-diamidino-2-phenylindole (Molecular Probes), Goat anti-Iba1 (Abcam), Alexa Fluor® 594 Goat anti-rabbit IgG (Molecular Probes), anti-CD31 (Abcam), anti-cytokeratin 13 (Abcam) were purchased.

2.2. Animals

The experimental procedure is described in Fig. 1. All animal procedures followed the standard ACUC (Animal Care and Use Committee) approved protocol (Johns Hopkins University). Laparotomy was conducted on pregnant rabbits at gestational day 28 (G28, term pregnancy 31 days) under general anesthesia (2–3% isoflurane by mask). Saline containing 6000EU of *Escherichia coli* endotoxin (*Escherichia coli* serotype O127:B8, Sigma Aldrich) (Endotoxin) or equivalent volume of saline alone (Control) was distributed equally (100 μL per injection site) and injected along the length of the uterus as previously described by our group. Immediately after this, 50 μL of Cy5-labeled D-OH or Cy5-labeled D-COOH (concentration of 12 mg/mL) were injected intra-amniotically into each gestational sac along the right uterine horn using a 30G needle (IA-Dendrimer). This would result in an individual fetal dose of ~20 mg/kg assuming a fetal weight of about 30 g. This dose was based on our previous study of intravenous injection of D-NAC in newborn rabbits, where dendrimer was administrated at doses ranging from 5.5 mg/kg to 55 mg/kg [21]. We also take into account that intra-amniotic injection is similar to oral administration, since the fetus swallows the amniotic fluid. The gestational sacs along the left uterine horn were injected with saline alone and served as internal controls (IA-Saline). As a result, 4 different groups were created in the study (as demonstrated in Fig. 1), namely (1) fetuses with endotoxin treatment and intra-amniotic (IA) dendrimer injection **(Endotoxin, IA-Dendrimer)**; (2) fetuses with endotoxin treatment and intra-amniotic saline injection **(Endotoxin, IA-Saline)**; (3) fetuses with control saline (Sham) treatment and intra-amniotic dendrimer injection **(Sham, IA-Dendrimer)**; (4) fetuses with control saline treatment and with intra-amniotic saline exposure **(Sham, IA-Saline)**. Dendrimer used in these 4 groups were either D-OH-Cy5 or D-COOH-Cy5. Routine closure was performed and the dams were recovered in individual cages. Cy5-labeled dendrimer solution diffused quickly in the amniotic fluid within 1 to 3 s. No indications of leakage were seen during or post injection

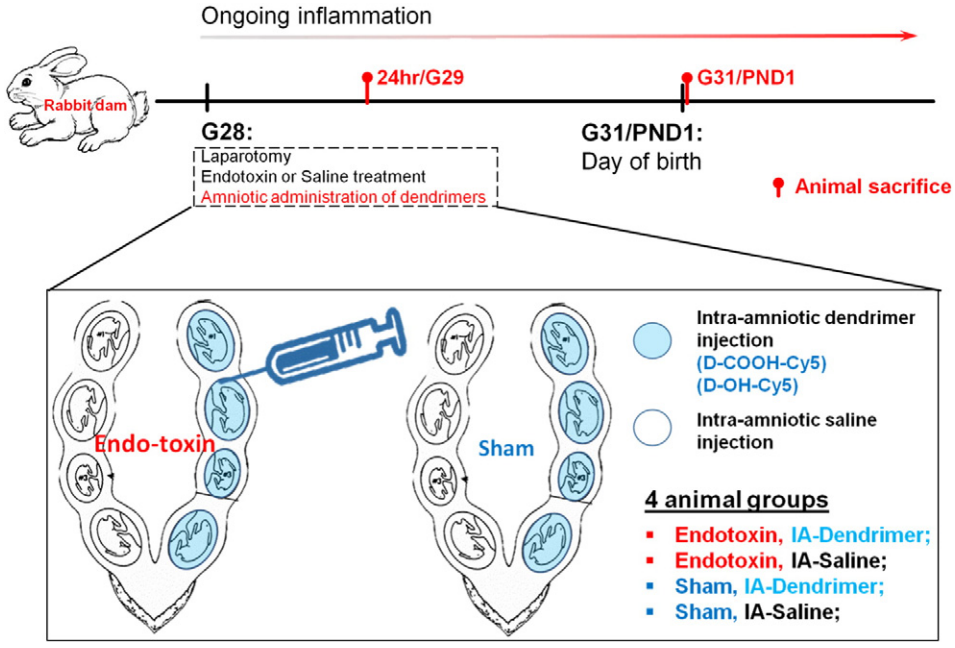

Fig. 1. Flow chart demonstrating surgery procedures designed in this experiment. Endotoxin or saline was administrated at G28 during the laparotomy, followed with intra-amniotic administration of dendrimer (Cy5-labeled D-OH or D-COOH) or saline. Animals were sacrificed at selected time points (*i.e.* G29 and G31/PND1 post dendrimer administration) for biodistribution and immunohistochemistry evaluation. BOX: Graphic explanation of 4 sample groups in this study. Namely (1) fetuses with endotoxin treatment and intra-amniotic (IA) dendrimer injection **(Endotoxin, IA-Dendrimer)**; (2) fetuses with endotoxin treatment and intra-amniotic saline injection **(Endotoxin, IA-Saline)**; (3) fetuses with control saline (Sham) treatment and intra-amniotic dendrimer injection **(Sham, IA-Dendrimer)**; (4) fetuses with control saline treatment and with intra-amniotic saline exposure **(Sham, IA-Saline)**.

(Supplementary Fig. 1). Procedures for animal sacrifice were previously described [21], and details of animal sacrifice and tissue collection are provided in the supplementary materials.

2.3. Dendrimer extraction procedure

The method for extraction and quantification of Cy5-labeled dendrimers is described previously [24]. Briefly, all tissue samples were defrosted before processing. Liquid samples (serum, urine, amniotic fluid) were diluted 10-fold in PBS and filtered through a 0.2 μm membrane before the measurements. For all tissue samples, 100 mg of tissue were dissected from each organ. For the intestinal tract, only the small intestine was dissected for quantification; for maternal organs, at least three samples per organ were dissected from each region to have an accurate representation of dendrimer accumulation. To obtain blood free and clear supernatants, samples were centrifuged for 15 min at 15,000 rpm and 4 °C using a 5424R, Eppendorf centrifuge. Supernatants were then analyzed by fluorescence spectroscopy.

2.4. Fluorescence spectroscopy

Fluorescence spectra of Cy5-labeled dendrimer extracts were recorded using a Shimadzu RF-5301 Spectrofluorometer. Calibration curves for Cy5-labeled dendrimers were constructed by recording the fluorescence intensity of Cy5-labeled dendrimers at emission wavelength of 662 nm or 665 nm, under the maximum of excitation at 645 nm. To maximize the intensity of emission, different sets of excitation and emission slit widths were applied for different dendrimer concentrations.

Spectra for each extract were recorded using different sets of excitation and emission slit widths, the one with the highest emission intensity was selected for quantification of dendrimer, applying a calibration curve obtained at the same conditions. To compensate for autofluorescence originating from the tissue matrix, intensities registered for control samples obtained from each specimen of non-treated animals were subtracted from the values observed for samples acquired from animals injected with Cy5-labeled dendrimers. All calculations were performed using Excel. Statistical analysis was performed using a Student's *t*-test.

2.5. Immunohistochemistry study of dendrimer accumulation and distribution

Fetal brains, fetal small intestine, and placenta were fixed with 4% PFA once they were harvested, followed by processing with gradient sucrose solutions (10%, 20%, 30%). Processed tissues were then cryosectioned with a Leica CM1850 cryostat (Leica Biosystems, USA). For all samples, DAPI was used to stain the nuclei. For fetal brain samples, goat anti-ionized calcium-binding adapter molecule 1 (anti-Iba1, primary antibody) and donkey anti-goat 594 (secondary antibody) were used to stain the microglia/macrophages. Anti-CD31 antibody (primary antibody) followed with donkey anti-mouse 488 (secondary antibody) was used to stain the blood vessels. For placenta samples, the placental villous structure was identified based on the staining of syncytiotrophoblast layer using anti-cytokeratin13 antibody (primary antibody) and donkey anti-mouse 488 (secondary antibody, Abcam). Images were obtained using Zeiss LSM 710 Meta Confocal Microscope (Carl Zeiss, USA).

3. Results

3.1. Preparation and characterization of Cy5-labeled D-OH and D-COOH dendrimers

The preparation of Cy5-labeled D-OH and D-COOH was followed with previously published protocols by our group with some modification [20,24] (details in supplementary materials). To confirm the preservation of neutral and negative surface charge of D-OH and D-COOH after partially functionalizing with amines, the size and ζ-potential of D-OH, amine functionalized D-OH, D-COOH, and amine functionalized D-COOH were measured using dynamic light scattering (DLS) and zeta-sizer, as shown in Table 1. After partially functionalizing with surface amines, the physical properties of D-OH and D-COOH were maintained, with a slightly increase in size (D-OH: from 4.4 ± 0.2 nm to 4.7 ± 0.3 nm; D-COOH: from 3.2 ± 0.4 nm to 3.8 ± 0.2 nm) and surface charge (D-OH: from 4.5 ± 0.1 mV to 6.6 ± 0.2 mV; D-COOH from −28.6 ± 0.7 to −21.8 ± 0.6).

Since Cy5-labeled dendrimers were administrated into the amniotic fluid and would probably circulate within this fluid for a long time, we tested the stability of Cy5-labeled dendrimers in both human and rabbit amniotic fluid. We found the Cy5-labeled dendrimers remained stable within amniotic fluid after 48 h of incubation period. HPLC analysis of each sample fraction before and after incubation showed that, in *human* amniotic fluid, ~8% of the Cy5 was released as free Cy5 over 48 h, whereas in the *rabbit* amniotic fluid ~4.5% of the Cy5 was released over 48 h. This suggests that the Cy5-labeled dendrimers were relatively stable in both human and rabbit amniotic fluid (Supplementary Fig. 2). Our quantification measures the fluorescence of the D-Cy5 recovered from the tissues.

3.2. D-OH and D-COOH partitioned into fetal systemic circulation and were transported into the maternal side

When compared to intravenous administration, intra-amniotic administration of dendrimers provides an opportunity for dendrimers to be exposed to the fetal gastrointestinal track (GI track) during the circulation of amniotic fluid within the amniotic sac. Hence, amniotic delivery would primarily represent 'oral delivery' of dendrimers. Based on this, we began assessing whether D-OH and D-COOH can pass through the intestinal wall and partition into the fetal systemic circulation. As expected, we observed that both D-OH and D-COOH transported across the epithelial layer of the intestinal villi and were detected along the inner wall of the intestinal villi at 24 h post administration (Fig. 2). This is likely a transient observation of the on-going process of dendrimer transport across the intestine epithelia layer. After this process is completed, these dendrimers will be absorbed by the fetus.

Surprisingly, the transport of dendrimers from amniotic fluid to fetal systemic circulation was rapid. In the biodistribution study performed at G29, the presence of dendrimers in major fetal and maternal organs was evaluated and expressed as percentage of injected dose per gram of tissue or per milliliter of liquid (%ID/g or mL). Most of the dendrimer injected had already transported out of the amniotic fluid, leaving only a limited amount of dendrimer (for D-OH, <3%/mL, for D-COOH, <0.5%/mL) present in the amniotic fluid (Fig. 3, top row). For dendrimer transported out of the amniotic fluid, it was either retained in fetal/maternal tissue or cleared out from maternal systemic circulation. We determined that ~20–30% D-OH and ~10% D-COOH were retained in the fetal side (Table 2), with most of the dendrimers accumulating in the fetal GI tract, lung and placenta (Fig. 3, bottom row). The high accumulation in the placenta was correlated with the finding that a significant amount of dendrimer was transported out from the fetal side and accumulated either in the maternal side (D-OH, 50–60%, Table 2) or excreted out from the urine (D-COOH, 70–80%, Table 2) (Supplementary Fig. 3).

Table 1
The Size, ζ-potential of G4-OH, amine modified G4-OH, G3.5-COOH, amine modified G3.5-COOH. The size and ζ-potential were obtained from dynamic light scattering.

Dendrimer	Size (Mean ± SEM) (nm)	ζ-potential ± SEM (mV)
G4-OH	4.3 ± 0.2	+4.5 ± 0.1
G4-OH–$(NH_2)_4$	4.7 ± 0.3	+6.6 ± 0.2
G3.5-COOH	3.2 ± 0.4	−28.6 ± 0.7
G3.5-COOH–$(NH_2)_4$	3.8 ± 0.2	−21.8 ± 0.6

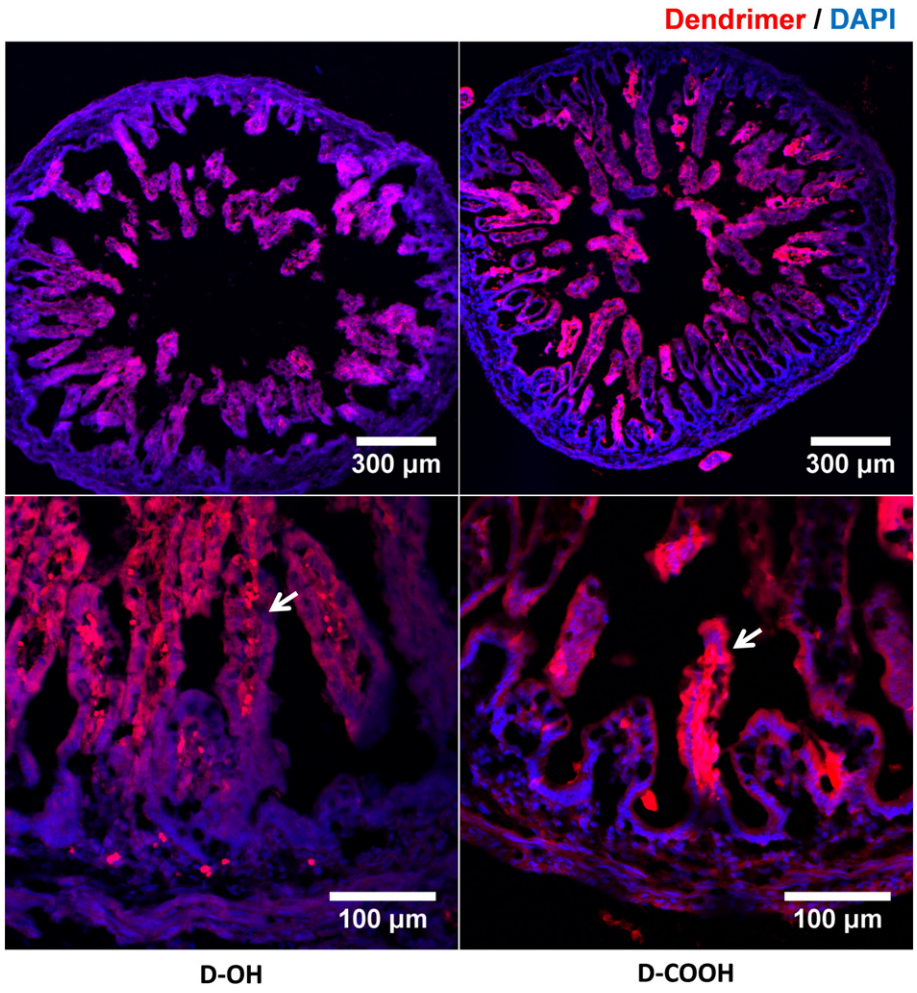

Fig. 2. Immunofluorescence images demonstrate D-OH and D-COOH distribution in the small intestine. As shown in both lower magnification (top) and higher magnification images (bottom), at 24 h (G29) post administration, dendrimers (D-OH and D-COOH) transported across epithelium layer of intestinal villi and presented at the inner side of intestinal villi, indicating the partition of both dendrimers into the blood capillaries. Red: D-OH or D-COOH; blue: DAPI. Scale bar: top: 300 μm, bottom: 100 μm.

The redistribution of the majority of dendrimer from amniotic fluid to both maternal and fetal compartments observed at G29, and excretion of the dendrimer in the maternal urine, indicates that dendrimer transport occurred within 24 h.

3.3. D-OH crossed BBB of endotoxin-treated fetus at G29, and showed co-localization in microglia, while D-COOH was restricted to the blood vessels in the brain

Since amniotic-administrated D-OH and D-COOH can both be orally absorbed by the fetus and enter into fetal systemic circulation, we sought to understand whether these dendrimers can reach the fetal brain parenchyma and target inflammatory cells. To identify whether these dendrimers can accumulate in the brain of an endotoxin-treated, injured fetus, we quantified the amount of brain accumulation of D-OH and D-COOH at G29 (24 h post dendrimer administration). Both dendrimers had a similar extent of total brain accumulation in the endotoxin-treated fetus at G29, with a slightly higher uptake for D-OH (0.28 μg/g of dry tissue) compared to D-COOH (0.22 μg/g of dry tissue) (Fig. 4A). However, further investigations using confocal microscopy revealed that the brain accumulation in the endotoxin treated fetus showed two distinctive distribution patterns between these two dendrimer platforms, attributable to the different surface charges of D-OH and D-COOH. As shown in Fig. 4B, at G29 (24 h after dendrimer administration), D-OH has less presence in the blood vessels. The relatively high background in the brain parenchyma around blood vessels and less co-localization with anti-CD31 (endothelial stain) indicated D-OH has already diffused across the BBB and distributed in the brain parenchyma around the periventricular region (PVR). On the contrary, D-COOH was only observed to be associated with blood vessels, with limited signal in the brain parenchyma. These findings suggest D-OH could cross the impaired BBB in the endotoxin-treated fetus and distribute within the brain parenchyma to reach target disease-associated cells.

3.4. D-OH and D-COOH did not accumulate in the brain parenchyma of sham fetus

There are several studies investigating the integrity of the BBB in the developing rodent brain. In healthy rabbits, the fetal BBB is thought to be intact prior to birth [25,26] and is more representative of the human BBB. We next sought to evaluate the distribution of both dendrimers in a sham fetus ('healthy' surgical control) to ensure that the BBB at this age is not leaky to dendrimer in 'healthy' fetuses. Given that sham fetuses were not exposed to endotoxin during their gestation period, their BBB should be intact relative to an endotoxin-treated fetus. As a result, although there was D-OH accumulation in the brain of sham fetus (Fig. 5A), D-OH was mainly associated with the blood vessels, and

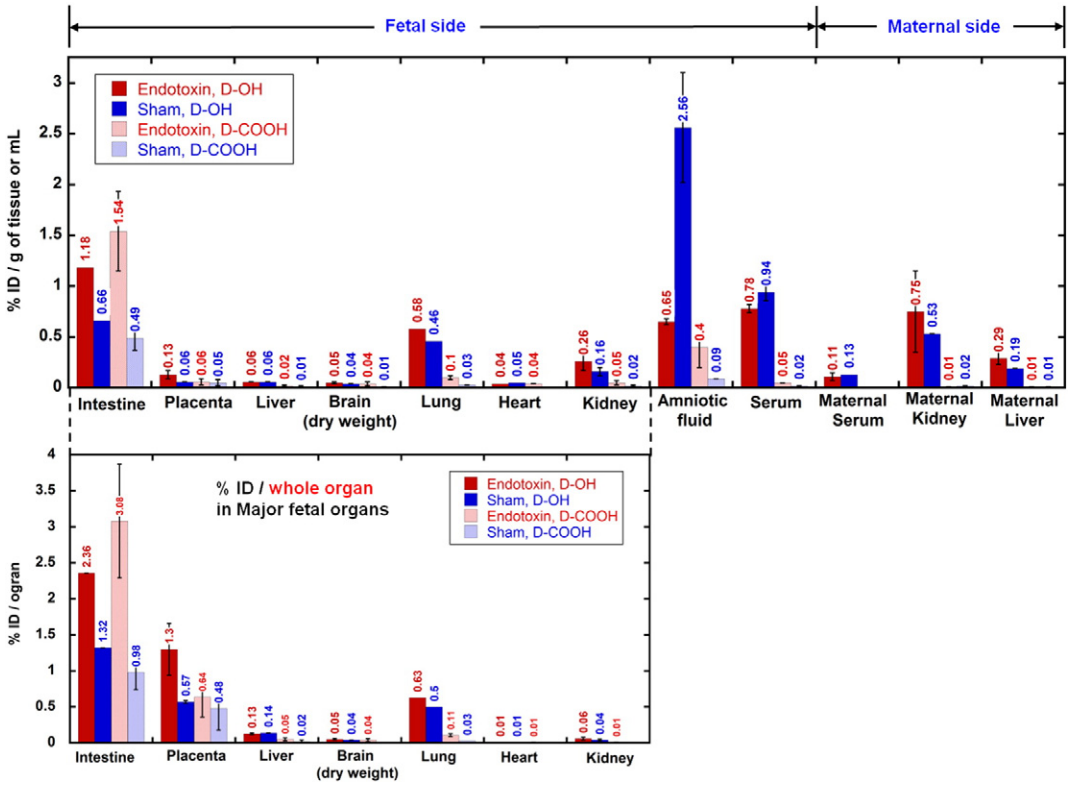

Fig. 3. Biodistribution of dendrimers (D-OH, indicated by solid columns and D-COOH, indicated by shaded columns) at 24 h post intra-amniotic administration in endotoxin groups (red columns) and sham groups (blue columns). Biodistribution is expressed as % injected dose per gram of tissue or milliliter of fluid [%ID/g of tissue or mL] (top) and % injected dose per whole organ in major fetal organs [%ID/organ] (bottom). On fetal side, dendrimers were mostly accumulated in the intestine, placenta and lungs (bottom) which are directly related to the amniotic fluid transport.

was not present in the brain parenchyma (Fig. 5B). In contrast, D-COOH were neither associated with blood vessels nor present in the brain parenchyma.

3.5. D-OH selectively localized in 'activated' microglia in different stages of activation

We have previously shown that D-OH accumulates in microglia in PND1 kits with CP, following systemic administration [21,22]. To determine if similar microglial uptake was present at PND1 with *intra-amniotic* administration of D-OH, we investigated the uptake and presence of D-OH in microglia on PND1 following D-OH intra-amniotic administration on G28. We found PND1 (G31) kits with CP had pronounced microglial uptake of D-OH. In this rabbit model of CP, a progressive increase in activation of microglial cells has been demonstrated after treatment with endotoxin [27]. Interestingly, the D-OH microglial uptake also showed an increasing trend with time from G29 to PND1 (Fig. 6). At G29, traces of D-OH signal were observed within microglial cells around the lateral ventricle, while at G31/PND1, the D-OH signal in microglial cells in the same region intensified significantly. Our results suggest that the observed increasing D-OH uptake is strongly associated with the progressive activation and proliferation of microglial cells in this model. Moreover, a longer exposure of the fetus to the dendrimer because of recirculation may increase the amount of dendrimer available for uptake by the microglial cells. This data also demonstrates that D-OH administered intra-amniotically preterm remains in microglial cells in the postnatal period.

Table 2
Estimation of D-OH and D-COOH distribution and clearance at 24 h (G29) post administration.

Dendrimer	% of total injected dose		
	Fetal uptake	Maternal uptake	Maternal urine
D-OH	20–30%	50–60%	10–30%
D-COOH	10%	2%	70–80%

3.6. D-OH and D-COOH re-crossed the placenta and were detected in fetuses that did not have intra-amniotic dendrimer injection

In order to understand the transport of dendrimer from the maternal–fetal, and fetal-maternal compartments, fetuses along one uterine horn were injected with dendrimer in the amniotic fluid while the fetuses along the other horn received only saline in the amniotic fluid. We then evaluated dendrimers accumulation in all fetuses. At G29, we observed that both D-OH and D-COOH were not only absorbed by the fetuses, but also transported across the placental barrier and were present in maternal systemic circulation. The high accumulation of dendrimer in the maternal side indicates that the fetuses that were not exposed to the dendrimer intra-amniotically were now exposed to it from the maternal circulation. This was seen for both D-OH and D-COOH dendrimers and in fetuses with and without endotoxin exposure (Fig. 7A). Quantification of D-OH accumulation in the fetal serum of IA-Saline groups showed that D-OH serum levels were consistent with the IA-D-OH fetuses. However, in the IA-Saline fetuses, D-OH concentration in the amniotic fluid was extremely low compared to that of the IA-D-OH fetuses, indicating that D-OH could be transported from the fetus across the placental barrier to the maternal side, and then be transported across again into the systemic circulation of the *other* IA-Saline fetuses. Similarly, D-COOH displayed the same trend with lower total accumulation in the IA-Saline fetuses. To assess the extent of maternal to fetal transport, we determined the 'IA-Saline to IA-dendrimer ratio' in the same mother (assessed across many mothers), by normalizing the dendrimer concentration in IA-Saline groups to those

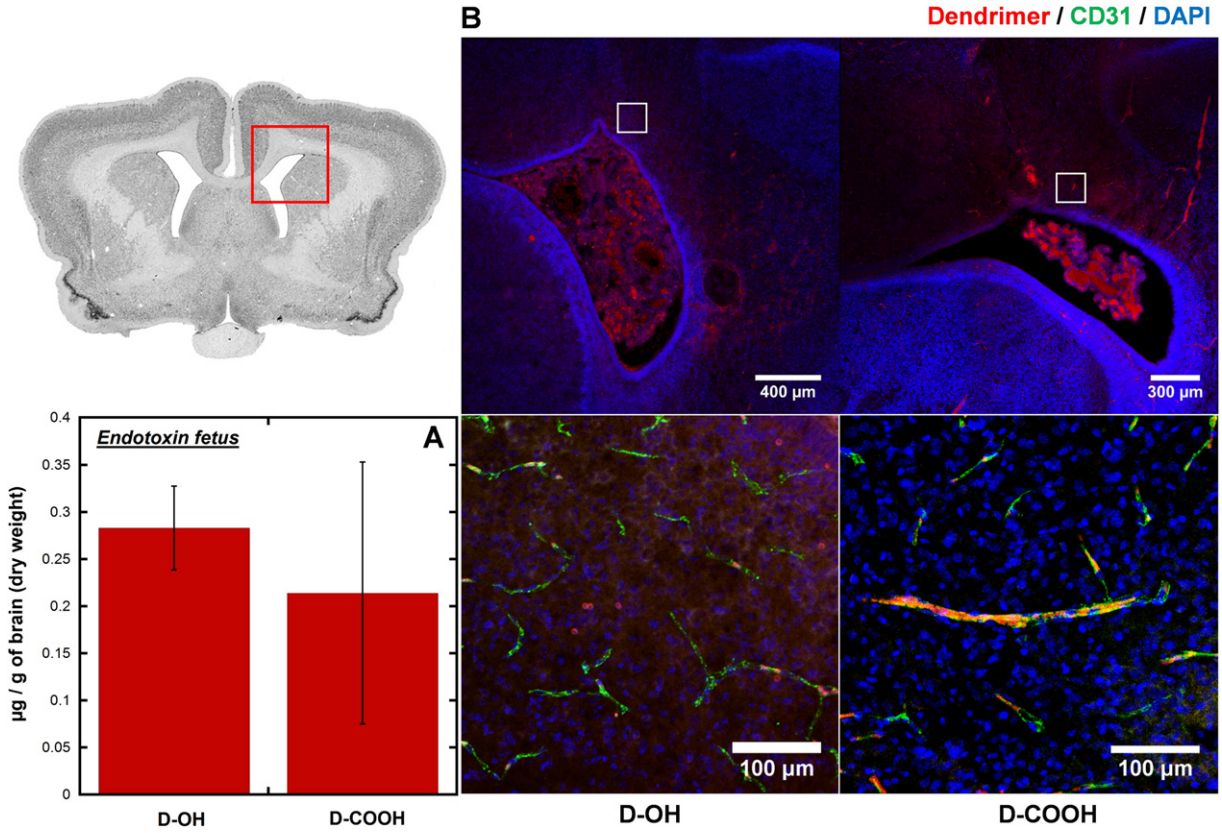

Fig. 4. Dendrimer accumulation and distribution in the brain of endotoxin-exposed fetuses at 24 h post intra-amniotic dendrimers administration. (A) Whole brain quantification shows both D-OH and D-COOH has similar accumulation in the brain of endotoxin-exposed fetus. (B) Immunofluorescence study shows different distribution of D-OH and D-COOH in the brain of endotoxin-exposed fetuses. D-OH escapes the impaired BBB and distributes in the brain parenchyma around the periventricular region; D-COOH is only observed to be restricted to the blood vessels. Red: D-OH or D-COOH; green: anti-CD31 labeled endothelial cells on BBB; blue: DAPI. Scale bar: top: 300 μm, bottom: 100 μm.

in the IA-dendrimer group (Fig. 7B):

IA – Saline to IA – dendrimer ratio = dendrimer concentration in IA – Saline group/dendrimer concentration in IA – denrdiemr group

The ratio was close to 1.0 in fetal organs and serum, indicating that the maternal to fetal transport was already close to equilibrium at 24 h post dendrimer administration. However, for the amniotic fluid and organs associated with amniotic fluid circulation and flow (such as intestine, kidney and lung), the IA-Saline to IA-dendrimer ratio was significantly lower, indicating that dendrimer accumulation in IA-Saline groups was primarily from maternal circulation. To further demonstrate the plausibility of placental dendrimer transport to the fetal side, we examined the dendrimer distribution in the placenta of IA-Saline groups (Fig. 8). Since the syncytiotrophoblast and cytotrophoblast layers serve as an interface between maternal blood and embryonic extracellular fluid, and thus control the exchange of dendrimer between maternal and fetal side [28], we stained these two layers and examined the dendrimer distribution. The presence of dendrimer in the syncytiotrophoblast and cytotrophoblast layer (labeled by anti-cytokeratin13) confirmed plausibility of placental dendrimer transport through the layer of syncytiotrophoblasts, crossing the placental barrier to the fetal side.

4. Discussion

We previously reported significant motor function improvement upon systemic dendrimer-NAC therapy, administered *after birth* in the rabbit model of CP [21]. However, since inflammation in the CNS often develops *in utero*, *prenatal therapy* could potentially prevent the injury at a much earlier stage. In this study, we demonstrate that dendrimers, when delivered by intra-amniotic administration in the prenatal period, can be absorbed by the fetus, cross the BBB in the fetal brain, and target microglial cells in the presence of inflammation. Our studies suggest that (1) dendrimers in the intra-amniotic fluid could be absorbed by the fetus and transported across the placental barrier into maternal systemic circulation; (2) the surface functionality of dendrimers influences their distribution and accumulation in the brain, and the more neutral D-OH was more effective in localizing in activated microglia in the brain when compared to the negatively charged D-COOH dendrimers; (3) the dendrimers could escape the amniotic sac, cross into maternal circulation, and re-cross the placental barrier from the maternal to the fetal side and were found even in the fetuses that did not initially receive intra-amniotic dendrimer injection.

4.1. Key factors that govern the targeting of dendrimers to neuroinflammation

The surface functionality of dendrimer affects dendrimers ability to target neuroinflammation. PAMAM dendrimers with amine surface functionality were not used in this study, due to their less potent tissue penetration [29], and higher neuronal [16,17] as well as systemic toxicity [14,30,31] compared to those with 'neutral' (OH) and 'anionic' (COOH) surface functionalities. We demonstrated neutral surface functionality is more desirable when designing a dendrimer-based conjugates for targeting inflammatory CNS disorders. This occurs due to a combination of the physiochemical properties of the dendrimer and the host characteristics including the presence of neuroinflammation. The damage of BBB provided a chance for molecules to extravasate from the leakage site, while the small size (~4.3 nm) and neutral surface charge enabled D-OH to efficiently cross the impaired BBB and diffuse within the extracellular matrix of the brain parenchyma and reach the

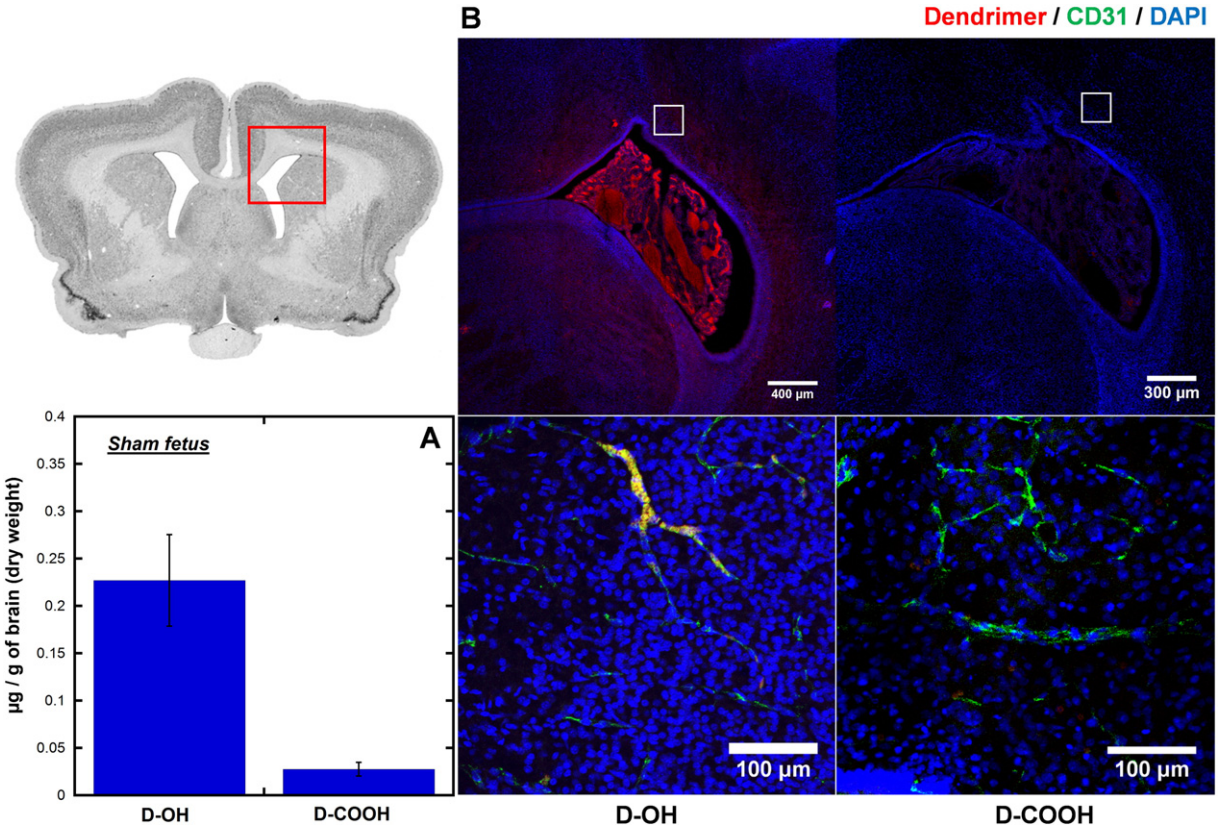

Fig. 5. Dendrimer accumulation and distribution in the brain of sham fetuses at 24 h post intra-amniotic dendrimers administration. (A) Whole brain quantification shows D-OH accumulates higher than D-COOH in the brain of sham fetuses. (B) Immunofluorescence study shows different distribution of D-OH and D-COOH in the brain of sham fetuses. D-OH is mainly restricted to the blood vessels, and is not presented in the brain parenchyma, while D-COOH is minimally present. Red: D-OH or D-COOH; green: anti-CD31 labeled endothelial cells on BBB; blue: DAPI. Scale bar: top: 300 μm, bottom: 100 μm.

microglial cells. The amount of brain accumulation of D-OH in this study (0.3 μg/g based on dose of 20 mg/kg) is in a similar order to that of systemic administrated D-OH (administrated at PDN1) (0.75 μg/g based on dose of 55 mg/kg). Given the significant therapeutic efficacy we achieved from systemically delivered D-OH based therapy, intra-amniotic route has the potential to deliver effective dose of therapeutics to the injured brain of CP kits. However, D-COOH was temporarily restricted to the blood vessels and did not demonstrated enough brain accumulation at G29, presumably due to the negative charge on the BBB surface [32].

In addition to desirable dendrimer physiochemical property and impaired BBB, microglial activation is another key factor that governs the target of dendrimers to microglia. This key factor has been previously demonstrated *ex vivo* in a brain slice-based platform [33]. In this *in vivo* study, we observed an increase dendrimer uptake with the progression of microglial activation. Specifically, microglial uptake at G31 (PND1) was greater than that of G29, likely due to the endotoxin-induced microglia activation that is more established at G31 than at G29 in this model [8,27,34].

4.2. Transport of intra-amniotically delivered dendrimers

Intra-amniotic delivery shares many similarities with oral delivery, the swallowing of amniotic fluid by the fetuses results in an initial exposure of the dendrimer to the fetal GI tract and the dendrimers were absorbed by the intestine villi as seen in Fig. 2 [36]. Although D-COOH has been reported to have better oral bioavailability, it has been noted that with high dendrimer concentrations (~300 mg/kg) and longer exposure times (>1 h), the GI absorption difference induced by dendrimer surface charge tends to be insignificant [13]. In our study, since dendrimers were continuously circulating within the amniotic fluid sac, even though D-COOH was reported to have better bioavailability, direct repeated exposure of fetal GI tract to high concentration of dendrimers in the amniotic fluid likely overwhelmed absorption of the GI tract, leading to no significant difference between D-OH and D-COOH in fetal uptake.

We observed differences of dendrimer accumulation in various tissues and liquids between endotoxin treated groups and sham groups, regardless of the dendrimer surface functionality. Endotoxin-treated groups generally showed a higher dendrimer accumulation in the tissues (varies between 2- and 3-fold higher depending on the tissue type), and lower retention in the amniotic fluid, when compared with the sham groups. This indicated an enhanced permeability in the GI track in the endotoxin-treated animals.

Dendrimer uptake through GI tract is a key pathway for dendrimer to be cleared from the amniotic sac. However, it is possible that the transport of dendrimers is associated with the kinetics of amniotic fluid flow, other dendrimer uptake pathways such as intra-membranous pathways [36], and the fast turnover rate of amniotic fluid among many species [37–39] might also contribute to the fast clearance of dendrimers from amniotic fluid.

4.3. Transport of dendrimers across blood-placenta barrier

Previous studies based on *ex vivo* perfusion of larger polystyrene nanoparticles in the placental tissue demonstrated that the ability for nanoparticles to cross the blood-placental barrier is size-dependent, with a higher transport efficiency for smaller sized nanoparticles [40]. We also showed in a previous *ex vivo* study the continuous transport of ~4 nm dendrimer-antipyrine conjugates (DA) from the maternal to

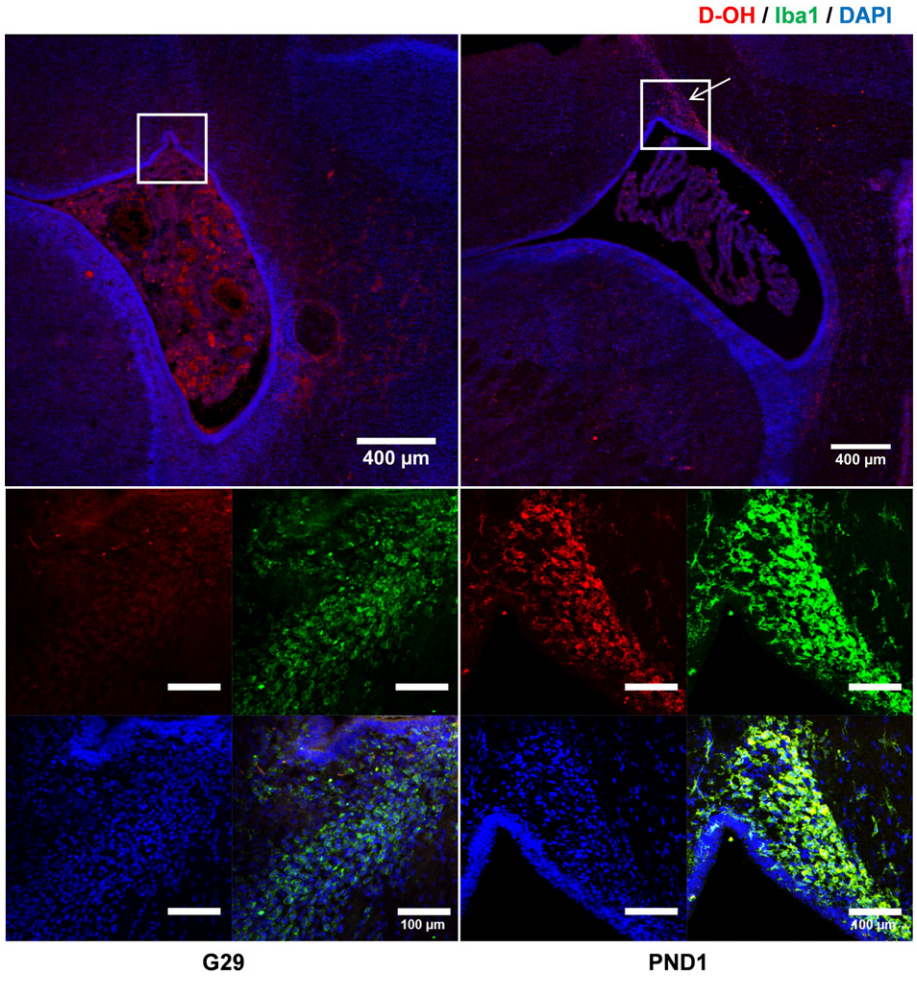

Fig. 6. D-OH microglia localization was accompanied with microglial activation. Low magnification images (top) showed that at G29, most D-OH distributed around the ventricle region, while at PND1, D-OH specifically accumulated at the ventricle horn (pointed out by the arrow). Magnification of the ventricle horn (bottom) showed that at G29, a hint of microglial localization was observed, while at PND1, D-OH was selectively localized within the activated microglial cells. Red: D-OH; green: anti-Iba1 labeled microglial cells; blue: DAPI. Scale bar: 400 μm.

the fetal side, with 4.1% of DA in the fetal circuit at 5 h post perfusion [41]. In this *in vivo* study, we observed transport of dendrimers across the placental barrier from the fetal to the maternal circulation and then back to the fetal side, which is indicated by the presence of dendrimer in the fetuses that did not initially receive intra-amniotic dendrimer. This is probably due to the normal rapid turnover of amniotic fluid *in vivo*. Amniotic fluid in humans has a turnover rate of approximately one day [42]. In addition, the fact that dendrimers were injected into several amniotic fluid sacs of the same dam expedited the accumulation of dendrimers in the maternal side. Since dendrimers appear to be transported across the placental barrier bi-directionally, fetuses from IA-Saline groups could receive dendrimers from the maternal source (dendrimer in maternal systemic circulation), while the fetuses from the dendrimer group (fetuses with dendrimer administration into amniotic fluid) received dendrimers from both the amniotic fluid and the back transport of dendrimer from the maternal source (Supplementary Fig. 4). Given that the dendrimer accumulation in the fetal brain showed similar uptake between intra-amniotic dendrimer exposed fetuses and intra-amniotic saline exposed littermates, it is possible that a large source of fetal brain accumulation resulted from transport of dendrimer from maternal to fetal circulation. It is likely that dendrimer in the amniotic fluid was absorbed into the splanchnic circulation from the fetal GI tract, which then combined with dendrimers transported across the placenta from the maternal circulation into the umbilical vessels. Some of this would be taken up into the brain while the rest would go back to the placenta through the umbilical arteries and then be transported back into the maternal circulation. As a result, high dendrimer accumulation was seen in the lung, intestine, or amniotic fluid which were directly exposed to intra-amniotic dendrimers, and in placenta, where a lot of dendrimer exchanges with the maternal side. It is possible that maternal intravenous administration will also lead to an adequate uptake in the brain. However, intra-amniotic administration may enable the use of a much lower dose of a dendrimer-drug when compared to maternal intravenous administration. It must be emphasized that these results are for hydroxyl-terminated generation-4 and carboxyl-terminated generation-3.5 PAMAM dendrimers. Given that the complex transport properties of intra-amniotically administered nanoparticles can depend on many physicochemical properties of the nanoparticles, caution must be exercised in generalizing these finding to all dendrimers.

5. Conclusion

We evaluated the potential of the PAMAM dendrimer platform for prenatal intra-amniotic treatment of the fetus for treatment of fetal neuroinflammation and prevention of perinatal brain injury. This could also be an intra-amniotic delivery platform for the treatment of other comorbidities associated with fetal inflammatory response syndromes. Further studies using dendrimer-drug conjugates will be required for evaluating efficacy of this drug delivery platform *via* this administration route.

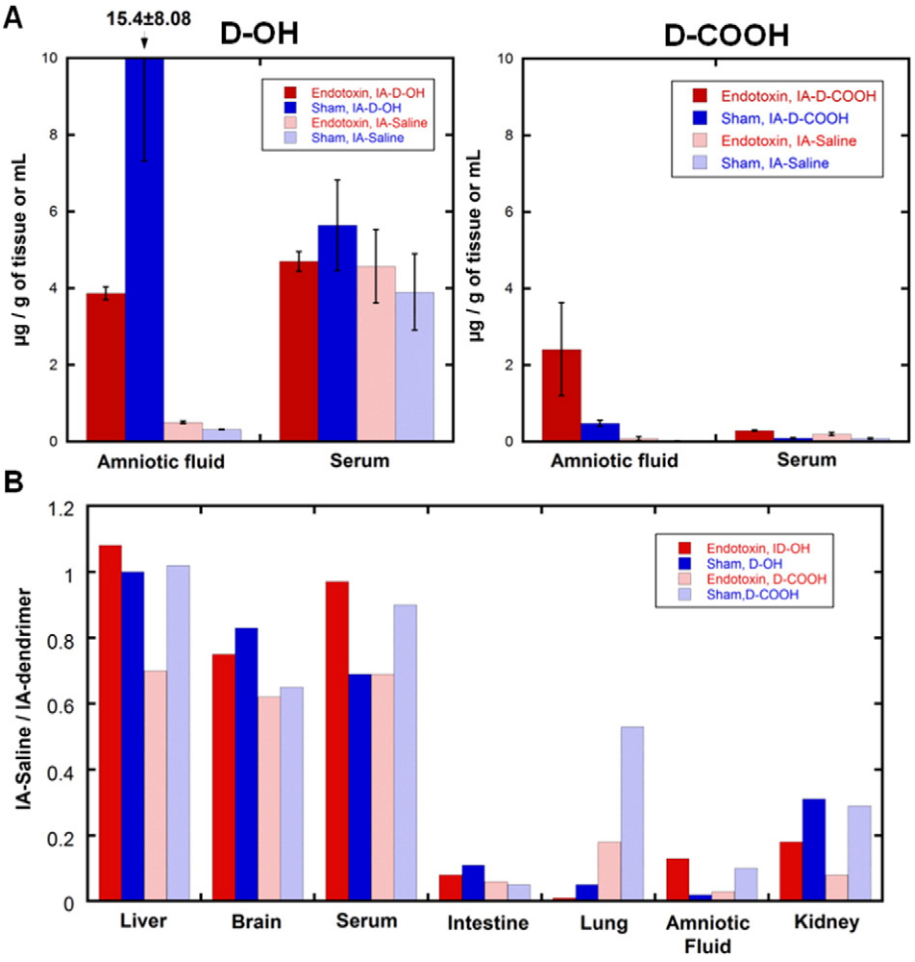

Fig. 7. Dendrimers distribution in fetus of IA-Dendrimer and IA-Saline groups. (A) Quantification of dendrimer accumulation in fetal serum and amniotic fluid shows IA-Dendrimer group (with intra-amniotic dendrimer administration, dark columns) and IA-Saline group (with intra-amniotic saline treatment, light columns) has similar dendrimer concentration in the fetal serum, but higher dendrimer concentration in the amniotic fluid of IA-Dendrimer group, and very low dendrimer concentration in the IA-Saline group for both endotoxin (red columns) and sham (blue columns) fetuses. (B) IA-Saline to IA-Dendrimer ratio was close to one in fetal brain, liver and serum, but low in fetal intestine, lung, amniotic fluid and kidney which are associated with the transport dynamics of amniotic fluid. D-OH: dark column, D-COOH: light column. Endotoxin: red column, CS: blue column.

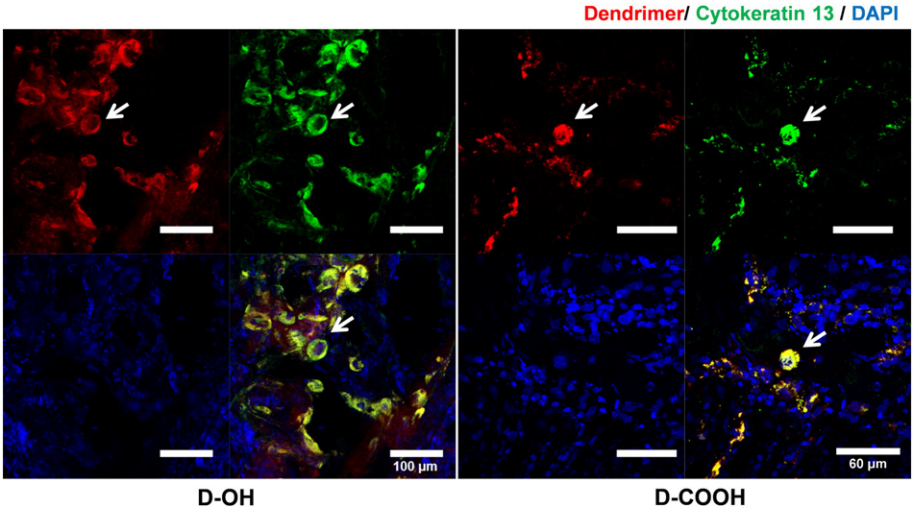

Fig. 8. Immunofluorescence study of dendrimer distribution in the placenta of *IA-Saline groups*. The presence of dendrimers in the syncytiotrophoblasts and cytotrophoblasts layer (labeled by anti-cytokeratin 13) of chorionic villi demonstrated the transport of dendrimers from maternal side across the blood-placenta barrier to the fetal side. Red: D-OH-Cy5 or D-COOH-Cy5; green: anti-cytokeratin 13 labeled syncytiotrophoblast and cytotrophoblast layer; blue: DAPI. Scale bar: 100 μm.

Acknowledgement

This study is supported in part by the Perinatology Research Branch, Division of Intramural Research, Eunice Kennedy Shriver National Institute of Child Health and Human Development (NICHD), NIH, and by NICHD R01HD069562 (S.K.), NIBIB 1R01EB018306 (R.M.K.), and NICHD 1R01HD076901 (R.M.K.). The funding source had no involvement in the research and/or preparation of the article. The authors would also like to acknowledge the Core Facility at the Wilmer Eye Institute at Johns Hopkins School of Medicine for providing the confocal microscope.

Appendix A. Supplementary data

Supplementary data to this article can be found online at http://dx.doi.org/10.1016/j.jconrel.2016.06.046.

References

[1] M. Bax, M. Goldstein, P. Rosenbaum, A. Leviton, N. Paneth, B. Dan, B. Jacobsson, D.P. Damiano, Executive committee for the definition of cerebral, proposed definition and classification of cerebral palsy, April 2005, Dev. Med. Child Neurol. 47 (2005) 571–576.
[2] L.A. Koman, B.P. Smith, J.S. Shilt, Cerebral palsy, Lancet 363 (2004) 1619–1631.
[3] C. Centers for Disease, Prevention, Economic costs associated with mental retardation, cerebral palsy, hearing loss, and vision impairment–United States, MMWR. Morb. Mortal. Wkly Rep. 53 (2004) (2003) 57–59.
[4] B.J. Stoll, N.I. Hansen, E.F. Bell, S. Shankaran, A.R. Laptook, M.C. Walsh, E.C. Hale, N.S. Newman, K. Schibler, W.A. Carlo, K.A. Kennedy, B.B. Poindexter, N.N. Finer, R.A. Ehrenkranz, S. Duara, P.J. Sanchez, T.M. O'Shea, R.N. Goldberg, K.P. Van Meurs, R.G. Faix, D.L. Phelps, I.D. Frantz, K.L. Watterberg, S. Saha, A. Das, R.D. Higgins, E.K.S.N. Inst, Neonatal outcomes of extremely preterm infants from the NICHD neonatal research network, Pediatrics 126 (2010) 443–456.
[5] A.T. Pakula, K.V. Braun, M. Yeargin-Allsopp, Cerebral palsy: classification and epidemiology, Phys. Med. Rehabil. Clin. 20 (2009) 427-+.
[6] R.L. Haynes, O. Baud, J. Li, H.C. Kinney, J.J. Volpe, R.D. Folkerth, Oxidative and nitrative injury in periventricular leukomalacia: a review, Brain Pathol. 15 (2005) 225–233.
[7] H. Hagberg, P. Gressens, C. Mallard, Inflammation during fetal and neonatal life: implications for neurologic and neuropsychiatric disease in children and adults, Ann. Neurol. 71 (2012) 444–457.
[8] B. Balakrishnan, E. Nance, M.V. Johnston, R. Kannan, S. Kannan, Nanomedicine in cerebral palsy, Int. J. Nanomedicine 8 (2013) 4183–4195.
[9] F. Zhang, Y.A. Lin, S. Kannan, R.M. Kannan, Targeting specific cells in the brain with nanomedicines for CNS therapies, J Control. Release (Dec 15, 2015), http://dx.doi.org/10.1016/j.jconrel.2015.12.013.
[10] R.M. Kannan, E. Nance, S. Kannan, D.A. Tomalia, Emerging concepts in dendrimer-based nanomedicine: from design principles to clinical applications, J. Intern. Med. 276 (2014) 579–617.
[11] S. Kannan, H. Dai, R.S. Navath, B. Balakrishnan, A. Jyoti, J. Janisse, R. Romero, R.M. Kannan, Dendrimer-based postnatal therapy for neuroinflammation and cerebral palsy in a rabbit model, Sci. Transl. Med. 4 (2012) 130ra146.
[12] I. Burd, F. Zhang, T. Dada, M.K. Mishra, T. Borbiev, W.G. Lesniak, H. Baghlaf, S. Kannan, R.M. Kannan, Fetal uptake of intra-amniotically delivered dendrimers in a mouse model of intrauterine inflammation and preterm birth, Nanomedicine-UK 10 (2014) 1343–1351.
[13] S. Sadekar, G. Thiagarajan, K. Bartlett, D. Hubbard, A. Ray, L.D. McGill, H. Ghandehari, Poly(amido amine) dendrimers as absorption enhancers for oral delivery of camptothecin, Int. J. Pharm. 456 (2013) 175–185.
[14] G. Thiagarajan, S. Sadekar, K. Greish, A. Ray, H. Ghandehari, Evidence of oral translocation of anionic G6.5 dendrimers in mice, Mol. Pharm. 10 (2013) 988–998.
[15] D. Hubbard, H. Ghandehari, D.J. Brayden, Transepithelial transport of PAMAM dendrimers across isolated rat Jejunal mucosae in Ussing chambers, Biomacromolecules 15 (2014) 2889–2895.
[16] S. Wang, Y. Li, J. Fan, Z. Wang, X. Zeng, Y. Sun, P. Song, D. Ju, The role of autophagy in the neurotoxicity of cationic PAMAM dendrimers, Biomaterials 35 (2014) 7588–7597.
[17] Y. Li, H. Zhu, S. Wang, X. Qian, J. Fan, Z. Wang, P. Song, X. Zhang, W. Lu, D. Ju, Interplay of oxidative stress and autophagy in PAMAM dendrimers-induced neuronal cell death, Theranostics 5 (2015) 1363–1377.
[18] G. Thiagarajan, K. Greish, H. Ghandehari, Charge affects the oral toxicity of poly(amidoamine) dendrimers, Eur. J. Pharm. Biopharm. 84 (2013) 330–334.
[19] S. Sadekar, H. Ghandehari, Transepithelial transport and toxicity of PAMAM dendrimers: implications for oral drug delivery, Adv. Drug Deliv. Rev. 64 (2012) 571–588.
[20] F. Zhang, P. Mastorakos, M.K. Mishra, A. Mangraviti, L. Hwang, J. Zhou, J. Hanes, H. Brem, A. Olivi, B. Tyler, R.M. Kannan, Uniform brain tumor distribution and tumor associated macrophage targeting of systemically administered dendrimers, Biomaterials 52 (2015) 507–516.
[21] S. Kannan, H. Dai, R.S. Navath, B. Balakrishnan, A. Jyoti, J. Janisse, R. Romero, R.M. Kannan, Dendrimer-based postnatal therapy for neuroinflammation and cerebral palsy in a rabbit model, Sci. Transl. Med. 4 (2012).
[22] H. Dai, R.S. Navath, B. Balakrishnan, B.R. Guru, M.K. Mishra, R. Romero, R.M. Kannan, S. Kannan, Intrinsic targeting of inflammatory cells in the brain by polyamidoamine dendrimers upon subarachnoid administration, Nanomedicine-UK 5 (2010) 1317–1329.
[23] E.A. Nance, G.F. Woodworth, K.A. Sailor, T.Y. Shih, Q.G. Xu, G. Swaminathan, D. Xiang, C. Eberhart, J. Hanes, A dense poly(ethylene glycol) coating improves penetration of large polymeric nanoparticles within brain tissue, Sci. Transl. Med. 4 (2012).
[24] W.G. Lesniak, M.K. Mishra, A. Jyoti, B. Balakrishnan, F. Zhang, E. Nance, R. Romero, S. Kannan, R.M. Kannan, Biodistribution of fluorescently labeled PAMAM dendrimers in neonatal rabbits: effect of neuroinflammation, Mol Pharmaceut. 10 (2013) 4560–4571.
[25] E.M. Cornford, M.E. Cornford, Nutrient transport and the blood-brain-barrier in developing animals, FASEB J. 45 (1986) 2065–2072.
[26] E.M. Cornford, L.D. Braun, W.H. Oldendorf, Developmental modulations of blood-brain-barrier permeability as an indicator of changing nutritional-requirements in the brain, Pediatr. Res. 16 (1982) 324–328.
[27] F. Saadani-Makki, S. Kannan, X. Lu, J. Janisse, E. Dawe, S. Edwin, R. Romero, D. Chugani, Intrauterine administration of endotoxin leads to motor deficits in a rabbit model: a link between prenatal infection and cerebral palsy, Am. J. Obstet. Gynecol. 199 (2008).
[28] K. Vahakangas, P. Myllynen, Drug transporters in the human blood-placental barrier, Br. J. Pharmacol. 158 (2009) 665–678.
[29] Y. Yang, S. Sunoqrot, C. Stowell, J. Ji, C.W. Lee, J.W. Kim, S.A. Khan, S. Hong, Effect of size, surface charge, and hydrophobicity of poly(amidoamine) dendrimers on their skin penetration, Biomacromolecules 13 (2012) 2154–2162.
[30] K. Greish, G. Thiagarajan, H. Herd, R. Price, H. Bauer, D. Hubbard, A. Burckle, S. Sadekar, T. Yu, A. Anwar, A. Ray, H. Ghandehari, Size and surface charge significantly influence the toxicity of silica and dendritic nanoparticles, Nanotoxicology 6 (2012) 713–723.
[31] H. Kulhari, D. Pooja, S.K. Prajapati, A.S. Chauhan, Performance evaluation of PAMAM dendrimer based simvastatin formulations, Int. J. Pharm. 405 (2011) 203–209.
[32] J. Bicker, G. Alves, A. Fortuna, A. Falcao, Blood-brain barrier models and their relevance for a successful development of CNS drug delivery systems: a review, Eur. J. Pharm. Biopharm. 87 (2014) 409–432.
[33] F. Zhang, E. Nance, Y. Alnasser, R. Kannan, S. Kannan, Microglial migration and interactions with dendrimer nanoparticles are altered in the presence of neuroinflammation, J. Neuroinflammation 13 (2016) 65.
[34] F. Saadani-Makki, S. Kannan, M. Makki, O. Muzik, J. Janisse, R. Romero, D. Chugani, Intrauterine endotoxin administration leads to white matter diffusivity changes in newborn rabbits, J. Child Neurol. 24 (2009) 1179–1189.
[36] M.H. Beall, J.P. van den Wijngaard, M.J. van Gemert, M.G. Ross, Amniotic fluid water dynamics, Placenta 28 (2007) 816–823.
[37] W.M. Gilbert, R.A. Brace, The missing link in amniotic fluid volume regulation: intramembranous absorption, Obstet. Gynecol. 74 (1989) 748–754.
[38] W.A. Lell, The relation of the volume of the amniotic fluid to the weight of the fetus at different stages of pregnancy in the rabbit, Anat. Rec. 51 (1931) 119–124.
[39] M.A. Underwood, W.M. Gilbert, M.P. Sherman, Amniotic fluid: not just fetal urine anymore, J. Perinatol. 25 (2005) 341–348.
[40] P. Wick, A. Malek, P. Manser, D. Meili, X. Maeder-Althaus, L. Diener, P.A. Diener, A. Zisch, H.F. Krug, U. von Mandach, Barrier capacity of human placenta for nanosized materials, Environ. Health Perspect. 118 (2010) 432–436.
[41] A.R. Menjoge, A.L. Rinderknecht, R.S. Navath, M. Faridnia, C.J. Kim, R. Romero, R.K. Miller, R.M. Kannan, Transfer of PAMAM dendrimers across human placenta: prospects of its use as drug carrier during pregnancy, J. Control. Release 150 (2011) 326–338.
[42] A.B. Modena, S. Fieni, Amniotic fluid dynamics, Acta Biomed. Ateneo Parmense 75 (Suppl. 1) (2004) 11–13.